

CERN-TH/2000-116
RAL-TR-2000-006
UR-1602
hep-ph/0004179

JET ACTIVITY IN $t\bar{t}$ EVENTS AND TOP MASS RECONSTRUCTION AT HADRON COLLIDERS

G. Corcella ¹, M.L. Mangano ² and M.H. Seymour ³

¹ Department of Physics and Astronomy, University of Rochester,
Rochester, NY 14627, U.S.A.

² CERN, Theory Division,
CH-1211, Geneva 23, Switzerland.

³ Rutherford Appleton Laboratory, Chilton,
Didcot, Oxfordshire. OX11 0QX. U.K.

Abstract

We analyse the impact of matrix-element corrections to top decays in HERWIG on several observables related to the jet activity in $t\bar{t}$ events at the Tevatron and at the LHC. In particular, we study the effects induced by the higher-order corrections to top decays on the top mass reconstruction using the recently proposed $J/\psi + \ell$ final states.

CERN-TH/2000-116
UR-1602
RAL-TR-2000-006
April 2000

1 Introduction

Top-quark and in general heavy-flavour production physics (see, for a review, [1]) is currently one of the main fields of investigation in both experimental and theoretical particle physics. At the next Run II of the Tevatron accelerator and, in the future, at the LHC [2] and at e^+e^- Linear Colliders [3], the production of a large amount of $t\bar{t}$ pairs will allow accurate studies of the top quark properties and an improved measurement of its mass.

The measurement of these properties will rely by-and-large on the accuracy of the theoretical modeling of the exclusive properties of the final states, for example jet distributions. Use of inclusive parton-level calculations, although resulting in the exact inclusion of the next-to-leading-order (NLO) contributions [4], is not sufficient to fully describe the effects associated with the large logarithms corresponding to soft or collinear parton emission. Calculations based on the fragmentation function formalism [5], where collinear logarithms can be resummed up to the NLO, are on the other hand too inclusive to allow a complete study of the final states. Monte Carlo event generators [6,7,8] are the best possible tool to perform the resummation of these enhanced logarithms, to simulate multiple radiation in high energy processes, and to provide a description of the hadronization transition leading to the final observable particles.

Inclusion of these higher-order corrections by the QCD event generators is done however in the soft/collinear approximation. Furthermore, the Monte Carlo evolution suppresses entirely emission of radiation inside some regions of the physical phase space ('dead zones') corresponding to hard and large-angle parton radiation. These regions are unfortunately sometimes crucial from the experimental point of view. Emission inside these dead zones can be performed using the exact amplitudes by following the method discussed in [9]. This method has been applied in the past to jet production in e^+e^- annihilation [10], in deep inelastic scattering [11] and, more recently, to the description of top decays [12] and of Drell-Yan processes [13]. Alternative approaches have also been proposed in the literature, see e.g. ref. [14].

In [12] a marked impact of matrix-element corrections to top decays was found for e^+e^- interactions slightly above the threshold for $t\bar{t}$ production. In this paper we wish to perform a similar analysis for top production and decay at hadron colliders and investigate the effect of the implemented hard and large-angle gluon radiation on jet observables and on the top mass reconstruction. As far as the top mass is concerned, we shall consider final states with leptons and J/ψ since the LHC experimentalists claim it is a favourite channel, with a systematic error no larger than 1 GeV [15], and we shall give more details on the analysis and the preliminary results presented in [16].

In Section 2 we briefly review the method applied in [12] to implement matrix-element corrections to the HERWIG description of top decays. In Section 3 we shall study phenomenologically-relevant jet observables at the Tevatron and at the LHC and investigate the impact of the improved treatment of top decays. In Section 4 we shall discuss the method of reconstructing the top mass by using final states with leptons and J/ψ and the effect of matrix-element corrections on the top mass measurement. In Section 6 we shall make some concluding remarks and comments on possible further improvements of the study here presented.

2 Matrix-element corrections to simulations of top decays

In the HERWIG Monte Carlo event generator, the top quark decay $t \rightarrow bW$ is performed in the top rest frame, as discussed in [17]. The top quark cannot emit soft gluons in its decay stage as it is at rest, while the b quark is allowed to radiate in the cone $0 < \theta_g < \pi/2$, θ_g being the soft-gluon emission angle relative to the direction of the b quark. The subsequent parton shower is performed following the prescription of the angular ordering [18]. The W hemisphere, corresponding to $\pi/2 < \theta_g < \pi$, is completely empty and the soft phase space is not therefore entirely filled by the HERWIG algorithm. In [17] the authors showed that neglecting the ‘backward’ gluon radiation correctly predicts the total energy loss, however problems are to be expected when dealing with angular distributions.

In [12] matrix-element corrections to the HERWIG simulation of top decays have been implemented: the missing phase space is populated according to a distribution obtained from the calculation of the exact first-order matrix element (hard correction), the shower in the already-populated region is corrected by using the exact amplitude any time a hardest-so-far emission is encountered in the evolution (soft correction).

Since the HERWIG dead zone includes part of the soft singularity, matrix-element corrections to top decays are not a straightforward extension of the method applied in [10,11,13]. The soft singularity has been avoided by setting a cutoff on the energy of the gluons which are radiated in the backward hemisphere by the b quark. As shown in [12], and discussed later on in this paper, the sensitivity to this cutoff is however very small.

In [12] e^+e^- interactions at a centre-of-mass energy $\sqrt{s} = 360$ GeV, slightly above the threshold for $t\bar{t}$ production, were considered. This is an ideal phenomenological environment to test the impact of the implemented corrections, with most of the radiation being associated to the top-decay stage. Three-jet events were analysed and a remarkable impact of matrix-element corrections was found when comparing different versions of HERWIG¹. The results of HERWIG 6.1 [19], the new version which includes also the improved treatment of top decays, were also compared to the ones obtained by the exact $\mathcal{O}(\alpha_S)$ matrix-element calculation of the process $e^+e^- \rightarrow t\bar{t} \rightarrow (bW^+)(bW^-)(g)$ [20]. While the authors of [20] had found serious discrepancies when comparing the exact $\mathcal{O}(\alpha_s)$ results with the ones of HERWIG before matrix-element corrections, good agreement was found in [12] after matrix-element corrections in the region of large energies and angles, where fixed-order calculations are reliable.

In [12] it was also shown that, although the fraction of events generated in the dead zone varies from about 2% to 4% when the cutoff changes from 5 GeV to 1 GeV, the dependence of phenomenological distributions on its chosen value is pretty negligible after one applies typical experimental cuts on the jet transverse energy $E_T > 10$ GeV and on the invariant opening angle between jets $\Delta R > 0.7$. The value $E_{\min} = 2$ GeV was then chosen as the default value and this value will be kept throughout this paper as well. In the following sections, we shall consider hadronic production of $t\bar{t}$ pairs and analyse the effect of matrix-element corrections to top decays on jet observables and on the top mass reconstruction at the Tevatron and at the LHC.

¹The latest public version HERWIG 5.9 had some errors in the treatment of top decays, which have been corrected in the intermediate version 6.0. In order to estimate the impact of matrix-element corrections, we therefore compare the versions 6.1 and 6.0

3 Jet activity in dilepton $t\bar{t}$ events

We start our analysis by considering inclusive jet observables. To emphasize the effect of the matrix element corrections to top decays, we confine ourselves to the case of leptonic decays of both W 's in each event. The most likely hard and well-separated jets are then those from the b and the \bar{b} . Extra radiation from either the initial state (ISR) or the top decay may give rise to extra jets (final state radiation from the produced $t\bar{t}$ pair tends to be small because of the large top mass). Interesting observables which may show the effects of the new HERWIG treatment of top decays are related to these extra jets, and in particular to the one with the largest value of E_T , the ‘third jet’.

We cluster jets according to the inclusive version of the k_T algorithm [21], setting a radius parameter $R = 0.5$ at the Tevatron and $R = 1$ at the LHC². We set a cutoff on the transverse energy of the resolved jets $E_T > 10$ GeV, and we study the following inclusive distributions: transverse energy E_T and rapidity η_3 of the third jet, the minimum invariant opening angle $\Delta R = \sqrt{\Delta\phi^2 + \Delta\eta^2}$ among the three hardest jets, the threshold variable d_3 of the k_T algorithm, according to which all events are forced to be three-jet-like. Finally, we consider the number of jets n_{jets} that pass the 10 GeV cut in transverse energy.

We start by comparing the Monte Carlo jet distributions before and after matrix-element corrections. To make the comparison more realistic, we normalize the plots to the expected integrated luminosities (2 fb^{-1} at $\sqrt{s} = 2$ TeV for the Tevatron Run II, and 10 fb^{-1} for 1 year of LHC low-luminosity running³), and smear the contents of a given bin with N events according to a Gaussian distribution with average N and standard deviation \sqrt{N} . Furthermore, to partially account for detector effects we smear the value of the reconstructed observables with a 10% resolution. The final jet distributions are plotted in Figs. 1-5.⁴

All observables show very small changes due to the matrix-element corrections. To quantify the residual differences, we performed a Kolmogorov–Smirnov test on the distributions, and evaluated the number of events necessary to establish the difference between the 6.0 and 6.1 distributions at 95% CL. The results of this test are shown in table 1. We see that at both machines a number of events of the order of $\approx 10^3 - 10^4$ is sufficient to see a difference in the shape of the two histograms. We therefore conclude that the effects of matrix-element corrections to top decays are in principle detectable at the LHC, where about 8×10^4 events per year are expected in the dilepton channel, while the foreseen statistics are too low at the Tevatron.

We conclude this Section by pointing out that the small differences detected in the case of inclusive third-jet observables are largely a consequence of the small fraction of events for which the matrix-element corrections are applied. We evaluated in fact that for the Tevatron energy only approximately 7% of events that contain a third jet required the evaluation of the matrix-element corrections to the top decays (the number is 6% for the LHC). We expect

²Such a choice is due to the relation between the R parameter of the k_T algorithm and the radius R_{cone} of the cone algorithm $R_{\text{cone}} \approx 0.75 \times R$ [22] and to the fact that the Tevatron experimentalist run a pure cone algorithm with $R_{\text{cone}} = 0.4$. For the LHC we shall nevertheless stick to the recommended value $R = 1$.

³Using total cross-sections of 7 pb and 830 pb for Tevatron and LHC [23], and assuming a conservative 1% overall efficiency and BR for the dilepton final states, this corresponds to approximately 150 [24] and 8×10^4 [25] events, respectively.

⁴With no smearing, the ΔR distributions at the Tevatron and at the LHC would have shown a sharp cutoff for $\Delta R = R$, as predicted by the k_T algorithm we have been using, but nevertheless the 10% smearing allows a small fraction of the jet events to have even $\Delta R < R$.

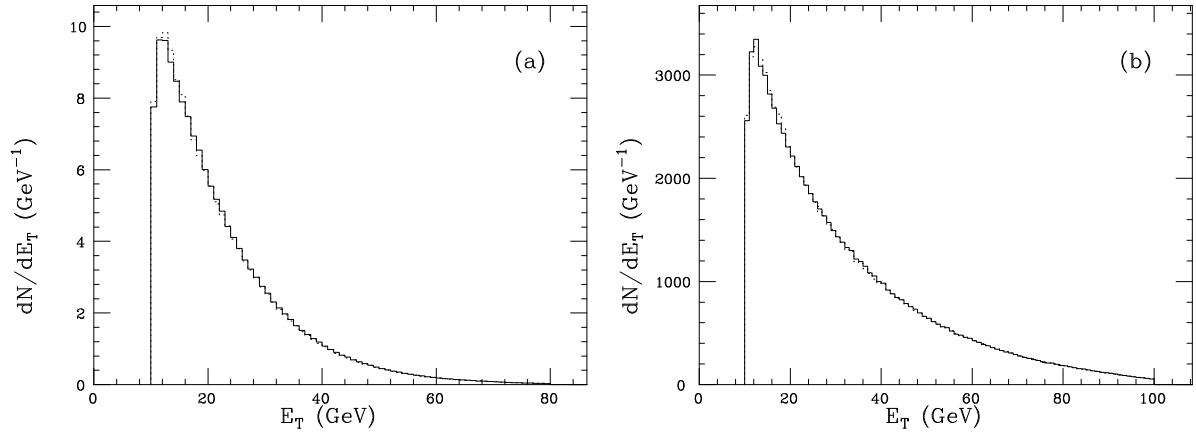


Figure 1: Transverse energy distribution of the third hardest jet at the Tevatron (a) and at the LHC (b), according to HERWIG 6.1 (solid line) and 6.0 (dotted).

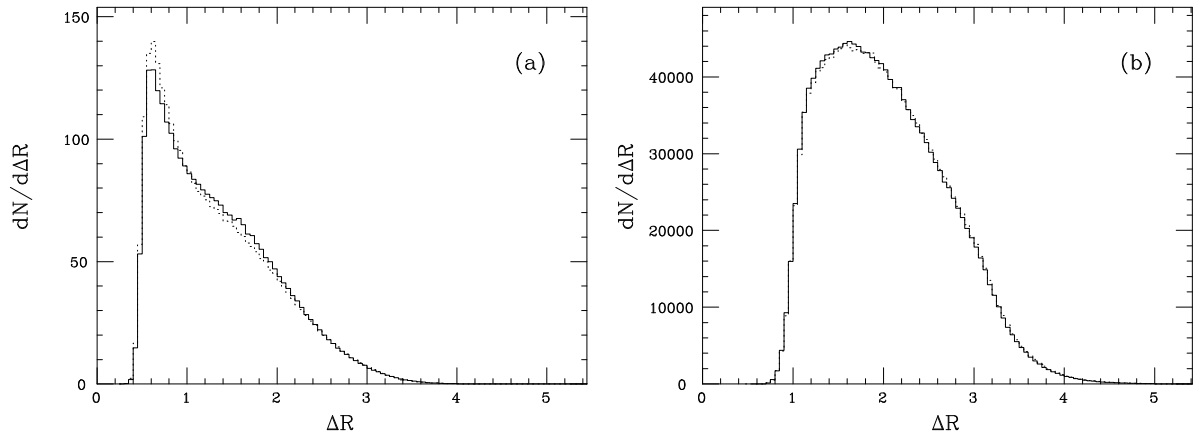


Figure 2: Distributions of the minimum invariant opening angle ΔR among the three hardest jets at the Tevatron (a) and at the LHC (b), according to HERWIG 6.1 (solid line) and 6.0 (dotted).

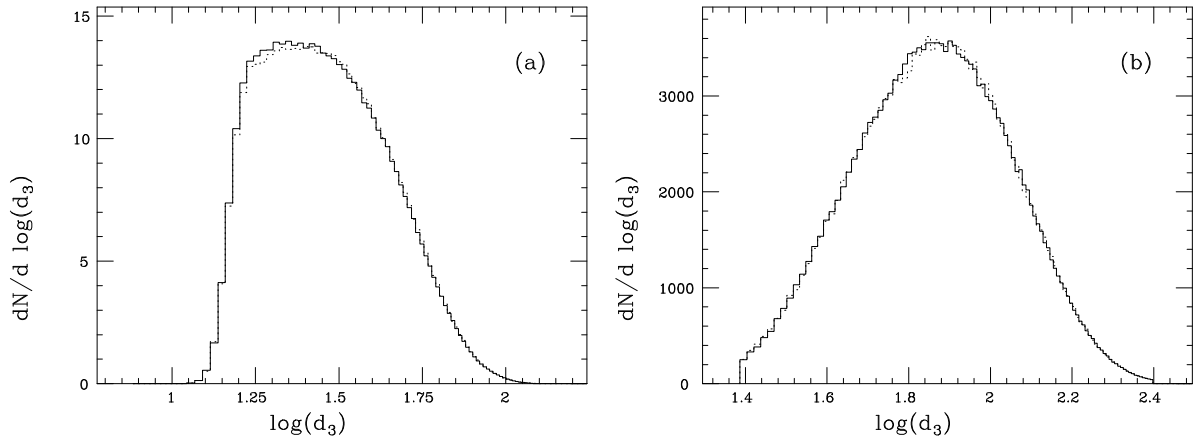


Figure 3: Distributions of the threshold variable d_3 for three-jet events at the Tevatron (a) and at the LHC (b), according to HERWIG 6.1 (solid line) and 6.0 (dotted).

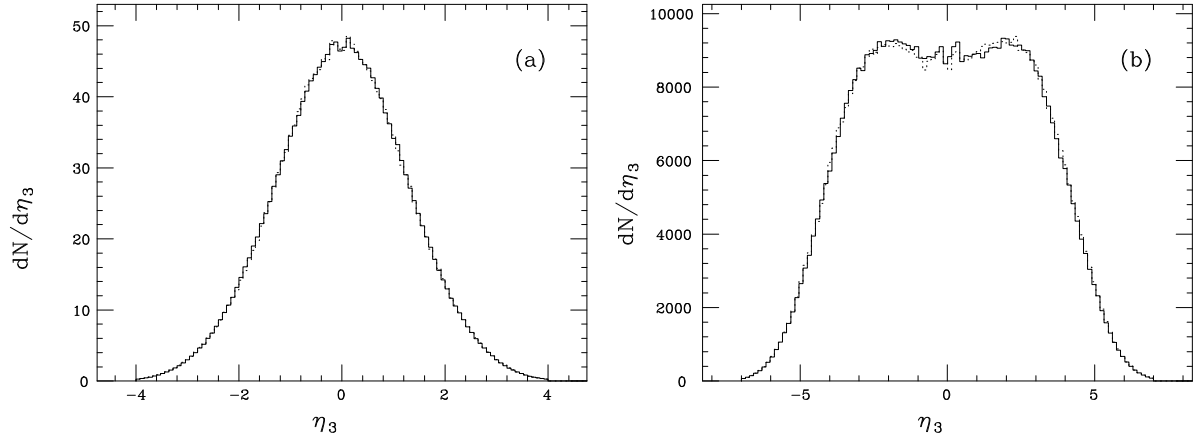


Figure 4: Distributions of the rapidity of the third hardest jet at the Tevatron (a) and at the LHC (b), according to HERWIG 6.1 (solid line) and 6.0 (dotted).

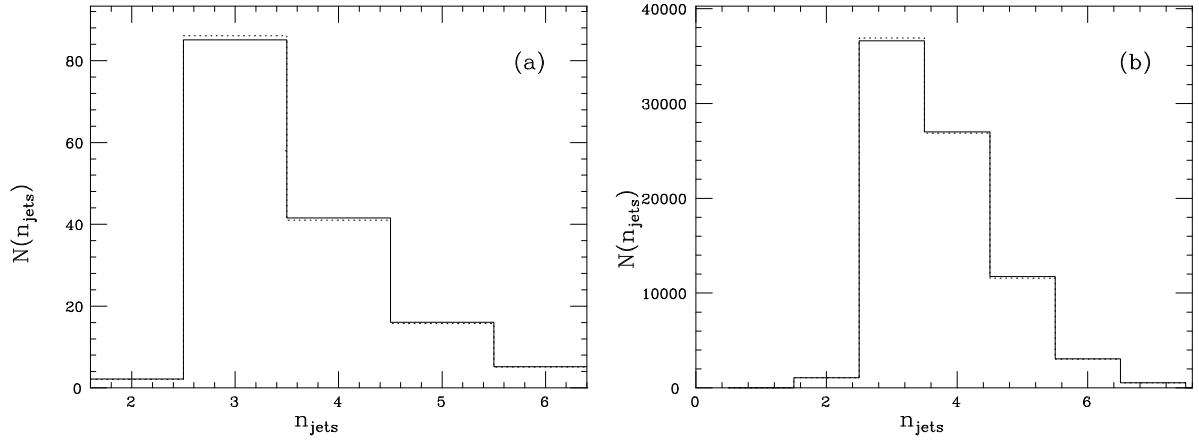


Figure 5: Number of jets passing the 10 GeV cut in transverse energy at the Tevatron (a) and at the LHC (b), according to HERWIG 6.1 (solid line) and 6.0 (dotted).

| observable | Tevatron | LHC |
|-------------|----------|------|
| E_T | 1000 | 1100 |
| $\log(d_3)$ | 3000 | 2700 |
| ΔR | 1100 | 4500 |
| η_3 | 5300 | 2500 |

Table 1: Number of $t\bar{t}$ events for which, according to the Kolmogorov test, the jet distributions using HERWIG 6.0 and 6.1 are different at the 95% confidence level.

that larger effects and differences will appear once the matrix-element corrections to the $t\bar{t}$ production process is included. This work is under way, along similar lines to vector boson production [13].

4 Top mass reconstruction

One observable for which the higher-order corrections described in this paper may induce relevant changes is the invariant mass distribution of $J/\psi + \ell$ pairs from $t \rightarrow bW$ decays, with the J/ψ coming from the decay of a b hadron, and the isolated lepton from the decay of the W . This distribution was recently suggested [15] as a potential way of measuring the top mass during the high-luminosity phase of the LHC with experimental accuracies better than 1 GeV. The dominant source of experimental uncertainty is the statistical one, due to the strong suppression from the small branching ratios⁵. The shape of the $m_{J/\psi+\ell}$ distribution can be compared with a template of shapes parametrised by the top mass, and the value of m_t can therefore be fitted. The Lorentz invariance of the observable makes it completely independent of the details of the $t\bar{t}$ production mechanism, and of the structure of the ISR. Given that the spectrum of the leptons from the W decay is known very well, the dominant theoretical uncertainty comes therefore from the predictions for the spectrum of the J/ψ . This is obtained from the convolution of the energy spectrum of b hadrons in the top decay, with the spectrum of J/ψ 's in the b -hadron decay. In principle this second element can be measured with high accuracy over the next few years at the B -factories⁶.

We shall therefore concentrate here on the problem of the b -hadron spectrum in top decays, and investigate how the top mass measurement is affected by the matrix-element corrections to top decays in HERWIG. For simplicity, we shall analyse the $m_{B\ell}$ spectra (instead of the $m_{J/\psi+\ell}$ ones) obtained by running HERWIG with and without matrix-element corrections to top decays.

The Tevatron statistics will be too low to use this channel as a probe of the top mass. Nevertheless we shall present results for the Tevatron as well, to show that indeed the details of the production mechanism (which is mainly $q\bar{q} \rightarrow t\bar{t}$ at the Tevatron and $gg \rightarrow t\bar{t}$ at the LHC) have no impact on the top mass determination. Since in $q\bar{q}$ annihilation the $t\bar{t}$ pair is always produced in a colour octet state, while in gg fusion it may come either in a colour singlet or colour octet state, this comparison will indicate that non-perturbative corrections to the $m_{B\ell}$ mass spectrum are very weakly dependent on the details of the colour-neutralization model in the MC.

We generate $t\bar{t}$ samples using HERWIG 6.0 and 6.1 and plot the $m_{B\ell}$ spectra for different values of m_t . We then evaluate the average value and the standard deviation of our distributions, the differences in the average values $\langle m_{B\ell} \rangle$ and the corresponding statistical errors. In Fig. 6 the $m_{B\ell}$ spectra are plotted for $m_t = 175$ GeV, at the Tevatron and at the LHC, before and after matrix-element corrections, while in Fig. 7 one can find the distributions at the LHC, according to HERWIG 6.1, for $m_t = 171$ GeV and $m_t = 179$ GeV. In tables 2 and 3 we summarize the results of our statistical analysis. We observe a systematic shift of about 800 – 900 MeV towards lower values of $\langle m_{B\ell} \rangle$ after matrix-element corrections to top decays.

⁵Ref. [15] estimates a sample of approximately 10^3 events in one year of high luminosity running at the LHC, $\mathcal{L} = 10^5 \text{ pb}^{-1}$, for a production cross section $\sigma_{\text{LHC}}(t\bar{t}) = 833 \text{ pb}$ and a total branching fraction $B = 5.3 \times 10^{-5}$, using the current expectations for tracking and reconstruction efficiencies.

⁶Although small corrections are expected to be needed for this application, due to the different composition of b -hadrons in top decays relative to that in the decays of the $\Upsilon(4S)$.

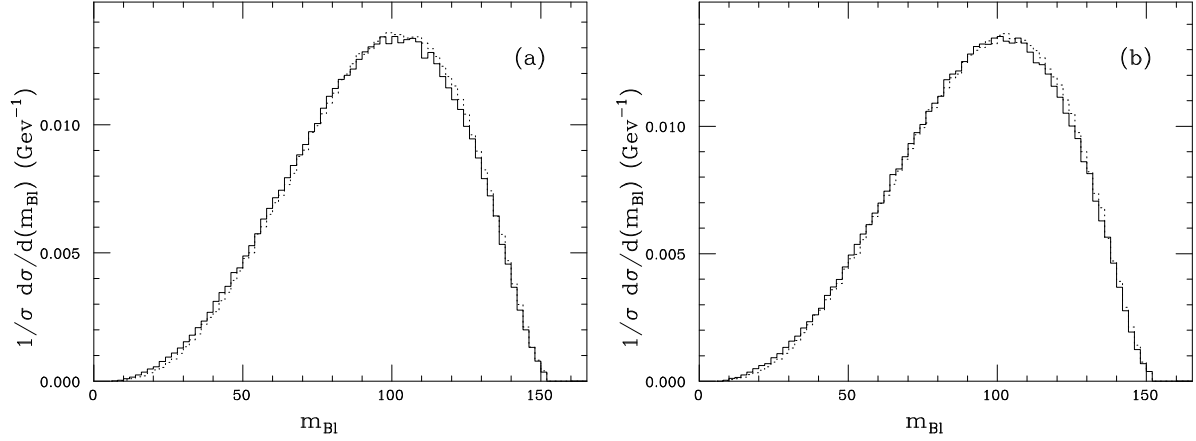


Figure 6: Invariant mass of the B -lepton system at the Tevatron (a) and at the LHC (b) for $m_t = 175$ GeV, according to HERWIG 6.0 (dotted) and 6.1 (solid).

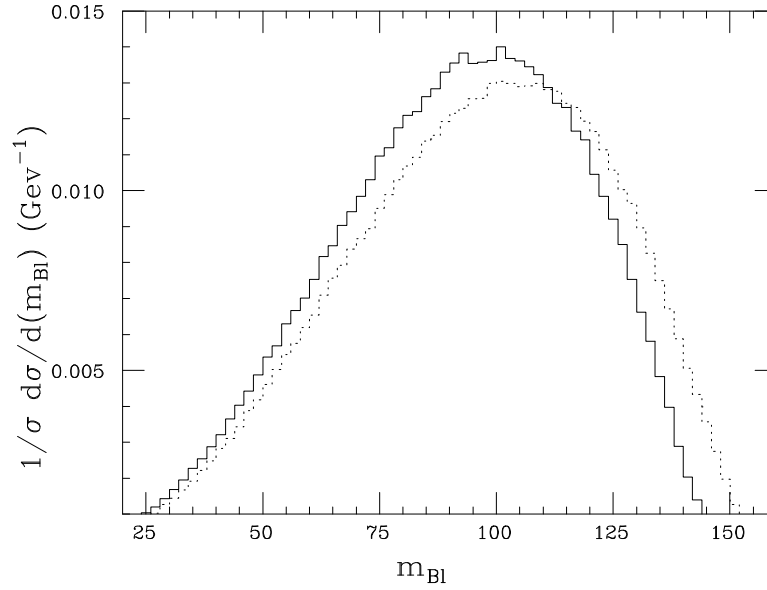


Figure 7: Invariant mass distributions according to HERWIG 6.1 at the LHC for $m_t = 171$ GeV (solid) and 179 GeV (dotted).

| m_t | $\langle m_{B\ell} \rangle^{6.1}$ | $\sigma(6.1)$ | $\langle m_{B\ell} \rangle^{6.0}$ | $\sigma(6.0)$ | $\langle m_{B\ell} \rangle^{6.0} - \langle m_{B\ell} \rangle^{6.1}$ |
|---------|-----------------------------------|---------------|-----------------------------------|---------------|---|
| 171 GeV | 91.18 GeV | 26.51 GeV | 92.06 GeV | 26.17 GeV | (0.873 ± 0.037) GeV |
| 173 GeV | 92.31 GeV | 26.90 GeV | 93.22 GeV | 26.58 GeV | (0.912 ± 0.038) GeV |
| 175 GeV | 93.41 GeV | 27.29 GeV | 94.38 GeV | 26.94 GeV | (0.972 ± 0.038) GeV |
| 177 GeV | 94.65 GeV | 27.73 GeV | 95.45 GeV | 27.33 GeV | (0.801 ± 0.039) GeV |
| 179 GeV | 95.64 GeV | 28.00 GeV | 96.63 GeV | 27.60 GeV | (0.984 ± 0.039) GeV |

Table 2: Results at the Tevatron for different values of m_t .

| m_t | $\langle m_{B\ell} \rangle^{6.1}$ | $\sigma(6.1)$ | $\langle m_{B\ell} \rangle^{6.0}$ | $\sigma(6.1)$ | $\langle m_{B\ell} \rangle^{6.0} - \langle m_{B\ell} \rangle^{6.1}$ |
|---------|-----------------------------------|---------------|-----------------------------------|---------------|---|
| 171 GeV | 91.13 GeV | 26.57 GeV | 92.02 GeV | 26.24 GeV | (0.891 ± 0.038) GeV |
| 173 GeV | 92.42 GeV | 26.90 GeV | 93.26 GeV | 26.59 GeV | (0.844 ± 0.038) GeV |
| 175 GeV | 93.54 GeV | 27.29 GeV | 94.38 GeV | 27.02 GeV | (0.843 ± 0.039) GeV |
| 177 GeV | 94.61 GeV | 27.66 GeV | 95.46 GeV | 27.33 GeV | (0.855 ± 0.039) GeV |
| 179 GeV | 95.72 GeV | 28.04 GeV | 96.51 GeV | 27.67 GeV | (0.792 ± 0.040) GeV |

Table 3: As in table 1, but for the LHC.

Furthermore, the results at the Tevatron are the same as the ones at the LHC, to within 150 MeV. Using the Kolmogorov–Smirnov test, we find that about $N_{\text{eff}} \simeq 6000$ reconstructed final states are sufficient to verify that the shapes of the 6.1 and the 6.0 distributions are different at the confidence level of 95%; one year of high-luminosity run would nevertheless allow one to distinguish the two distributions at 70% confidence level.

We studied the dependence of our results on the chosen infrared cutoff for the energy of the gluons emitted in the dead zone, which was discussed in Section 2. We find a negligible variation: at the LHC, and for $m_t = 175$ GeV, we find $\langle m_{B\ell} \rangle = 93.78, 93.54$ and 93.47 GeV for $E^{\text{cutoff}} = 1, 2$ and 5 GeV, respectively. The distributions in Fig. 8, obtained for $m_t = 175$ GeV and different values of E^{cutoff} , are essentially identical.

If we set a cut $m_{B\ell} > 50$ GeV on the invariant mass, to reduce the sensitivity to low-mass tails possibly affected by backgrounds, we find the results summarized in tables 4 and 5 for the Tevatron and the LHC respectively. Once we cut off part of the spectrum, it is to be expected that we find higher values for $\langle m_{B\ell} \rangle$ and lower values for the differences $\langle m_{B\ell} \rangle^{6.0} - \langle m_{B\ell} \rangle^{6.1}$, which are indeed now of about 400 – 500 MeV. Once again the shifts at the Tevatron and at the LHC are of similar size, within 150 MeV.

In order to evaluate the impact of the found discrepancies on the top mass, we perform a linear fit of the $\langle m_{B\ell} \rangle$ distribution as a function of m_t , by means of the least square method. We find, after considering all the $m_{B\ell}$ values:

$$6.1 : \langle m_{B\ell} \rangle = 0.563 m_t - 5.087 \text{ GeV}, \quad \epsilon(\text{GeV}) = 0.046 \text{ (Tevatron)}; \quad (1)$$

$$6.0 : \langle m_{B\ell} \rangle = 0.568 m_t - 5.139 \text{ GeV}, \quad \epsilon(\text{GeV}) = 0.023 \text{ (Tevatron)}; \quad (2)$$

$$6.1 : \langle m_{B\ell} \rangle = 0.568 m_t - 6.004 \text{ GeV}, \quad \epsilon(\text{GeV}) = 0.057 \text{ (LHC)}; \quad (3)$$

$$6.0 : \langle m_{B\ell} \rangle = 0.559 m_t - 3.499 \text{ GeV}, \quad \epsilon(\text{GeV}) = 0.052 \text{ (LHC)}; \quad (4)$$

where ϵ is the mean square deviation in the fit. We see that the linear fit is very good, and

| m_t | $\langle m_{B\ell} \rangle^{6.1}$ | $\sigma(6.1)$ | $\langle m_{B\ell} \rangle^{6.0}$ | $\sigma(6.0)$ | $\langle m_{B\ell} \rangle^{6.0} - \langle m_{B\ell} \rangle^{6.1}$ |
|---------|-----------------------------------|---------------|-----------------------------------|---------------|---|
| 171 GeV | 95.98 GeV | 22.22 GeV | 96.43 GeV | 22.22 GeV | (0.476 ± 0.036) GeV |
| 173 GeV | 97.03 GeV | 22.64 GeV | 97.51 GeV | 22.68 GeV | (0.511 ± 0.034) GeV |
| 175 GeV | 98.08 GeV | 23.15 GeV | 98.59 GeV | 23.11 GeV | (0.514 ± 0.035) GeV |
| 177 GeV | 99.23 GeV | 23.58 GeV | 99.60 GeV | 23.53 GeV | (0.396 ± 0.035) GeV |
| 179 GeV | 100.13 GeV | 23.93 GeV | 100.63 GeV | 23.90 GeV | (0.560 ± 0.036) GeV |

Table 4: Results for the invariant mass $m_{B\ell}$ at the Tevatron for different values of m_t , once we select a sample with $m_{B\ell} > 50$ GeV.

| m_t | $\langle m_{B\ell} \rangle^{6.1}$ | $\sigma(6.1)$ | $\langle m_{B\ell} \rangle^{6.0}$ | $\sigma(6.0)$ | $\langle m_{B\ell}^{6.0} \rangle - \langle m_{B\ell}^{6.1} \rangle$ |
|---------|-----------------------------------|---------------|-----------------------------------|---------------|---|
| 171 GeV | 95.97 GeV | 22.24 GeV | 96.45 GeV | 22.26 GeV | (0.479 ± 0.036) GeV |
| 173 GeV | 97.09 GeV | 22.69 GeV | 97.56 GeV | 22.68 GeV | (0.479 ± 0.034) GeV |
| 175 GeV | 98.14 GeV | 23.12 GeV | 98.64 GeV | 23.15 GeV | (0.510 ± 0.035) GeV |
| 177 GeV | 99.16 GeV | 23.54 GeV | 99.62 GeV | 23.52 GeV | (0.466 ± 0.035) GeV |
| 179 GeV | 100.20 GeV | 23.96 GeV | 100.62 GeV | 23.90 GeV | (0.427 ± 0.036) GeV |

Table 5: Results for the invariant mass $m_{B\ell}$ at the LHC for different values of m_t , once we select a sample with $m_{B\ell} > 50$ GeV.

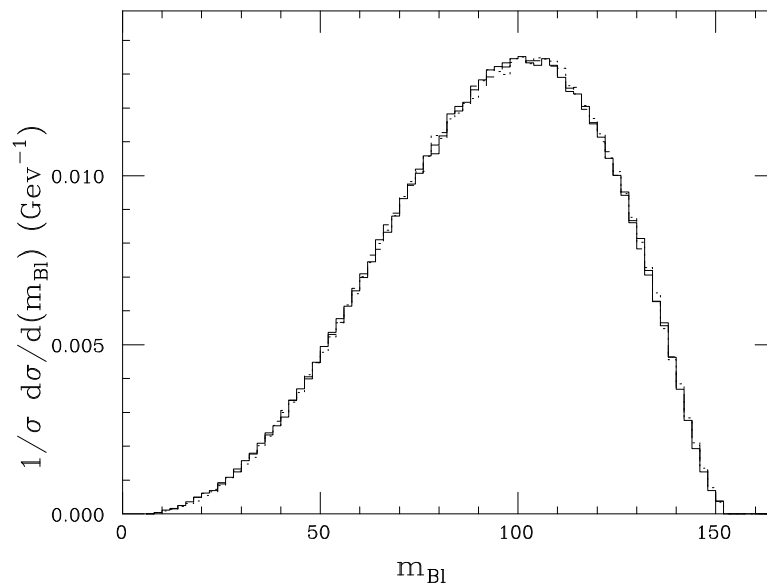


Figure 8: Invariant mass distributions according to HERWIG 6.1 for $m_t = 175$ GeV and a cutoff on the backward gluon energy equal to 1 GeV (dotted line), 2 GeV (solid) and 5 GeV (dashed).

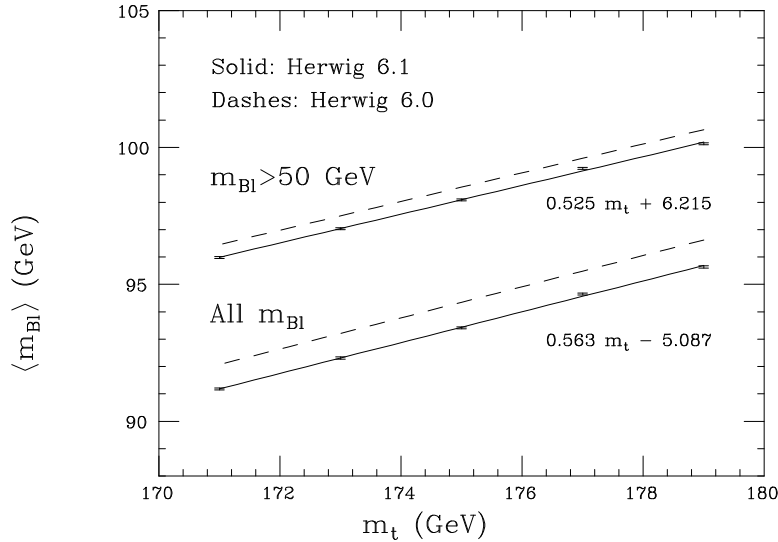


Figure 9: Results for the average invariant mass $\langle m_{B\ell} \rangle$ as a function of m_t at the Tevatron after a fit into a straight line. The solid and dashed lines refer to HERWIG 6.1 and HERWIG 6.0 respectively.

well within the required accuracy. The obtained fits are plotted in Figs. 9 and 10 at the Tevatron and at the LHC respectively. The error bars correspond to the statistical errors found on $\langle m_{B\ell}^{6.0} \rangle - \langle m_{B\ell}^{6.1} \rangle$, which, as can be seen from the figures, are significantly lower than the difference due to the implementation of matrix-element corrections to top decays. This means that the impact on the top mass is a physical effect and not just the result of statistical fluctuations.

Using these fits, and inverting the relation between $\langle m_{B\ell} \rangle$ and m_t , we find that for a given value of $\langle m_{B\ell} \rangle$ consistent with the range $171 \lesssim m_t \lesssim 179$, the values of m_t extracted using the two versions of HERWIG differ by 1.5 GeV, both at the Tevatron and at the LHC. This is a rather large value, competitive with the expected systematic error at the LHC, indicating that such corrections are relevant, and must be applied.

After setting a cut of 50 GeV on the $m_{B\ell}$ spectra, we obtain the following fits:

$$6.1 : \langle m_{B\ell} \rangle = 0.525 m_t + 6.125 \text{ GeV} , \epsilon(\text{GeV}) = 0.049 \text{ (Tevatron)} ; \quad (5)$$

$$6.0 : \langle m_{B\ell} \rangle = 0.524 m_t + 6.765 \text{ GeV} , \epsilon(\text{GeV}) = 0.022 \text{ (Tevatron)} ; \quad (6)$$

$$6.1 : \langle m_{B\ell} \rangle = 0.526 m_t + 5.974 \text{ GeV} , \epsilon(\text{GeV}) = 0.026 \text{ (LHC)} ; \quad (7)$$

$$6.0 : \langle m_{B\ell} \rangle = 0.520 m_t + 7.578 \text{ GeV} , \epsilon(\text{GeV}) = 0.040 \text{ (LHC)} . \quad (8)$$

The differences in the top mass extraction between the 6.0 and 6.1 versions from a given value of $\langle m_{B\ell} \rangle$ are now reduced to 1 GeV, smaller than for the fully inclusive distribution, but still significant relative to the overall accuracy goal of 1 GeV.

To conclude our study, we wish to investigate the dependence of our results on the hadronisation model used by HERWIG. We start by studying the invariant mass distribution of the lepton with the b quark, as opposed to the b -hadron. We do this by considering the HERWIG final state at the end of the perturbative evolution, just before the non-perturbative gluon-splitting phase which precedes the formation of the colour-singlet clusters, and the eventual hadronisation.

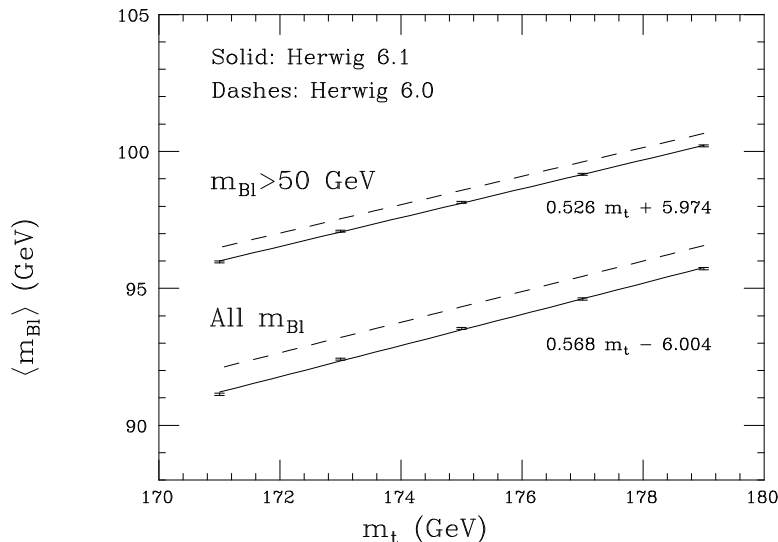


Figure 10: Results for the average invariant mass $\langle m_{B\ell} \rangle$ as a function of m_t at the LHC after a fit into a straight line. The solid and dashed lines refer to HERWIG 6.1 and HERWIG 6.0 respectively.

In Fig. 11 we plot the 6.0 and 6.1 distributions of the invariant mass of the b -lepton system for $m_t = 175$ GeV and the 6.1 ones at hadron- and parton-level. The results at parton level for different values of the top mass can be found in table 6. We find that, at fixed m_t , the average values of the parton-level invariant masses $\langle m_{b\ell} \rangle$ are larger than the ones after the hadronisation of the b quark, with differences between the 6.0 and the 6.1 version of the order about 600 – 700 MeV.

After a linear fit, we find the following relations:

$$6.1 : \langle m_{b\ell} \rangle = 0.640 m_t - 10.256 \text{ GeV} , \epsilon(\text{GeV}) = 0.050 . \quad (9)$$

$$6.0 : \langle m_{b\ell} \rangle = 0.646 m_t - 10.528 \text{ GeV} , \epsilon(\text{GeV}) = 0.033 \quad (10)$$

Given the values of the slopes, the shift in the extracted top mass between the two versions is now of about 1.0 GeV, compared to the 1.5 GeV after hadronisation.

As a whole, the non-perturbative contribution to the shape of the b -hadron spectra is therefore pretty important, as is already known in the case of Z^0 decays. Confidence in the accurate description of the non-perturbative phase should be gained from the study of the B -fragmentation function in Z^0 decays. Our study of the impact of matrix element corrections at the Tevatron and at the LHC suggests that non-perturbative corrections do not depend significantly on the production mechanism. This we also checked by performing a similar study in the case of e^+e^- production. We therefore expect that once a tuning of the non-perturbative b fragmentation function in HERWIG is achieved, using for example the latest high-precision SLD results [26], the results can be extended to the study of the $B\ell$ mass spectrum in top decays. Given the size of the mass shift induced by hadronisation (of the order of 8 GeV, as found by comparing Table 6 and 3), a control over the fragmentation function at a level better than 5% will have to be achieved in order to maintain this contribution to the theoretical systematics well below $\mathcal{O}(1 \text{ GeV})$. This should be possible, since the current size of the experimental uncertainty on $\langle x_B \rangle$ is at the level of $\sim 1\%$ [26].

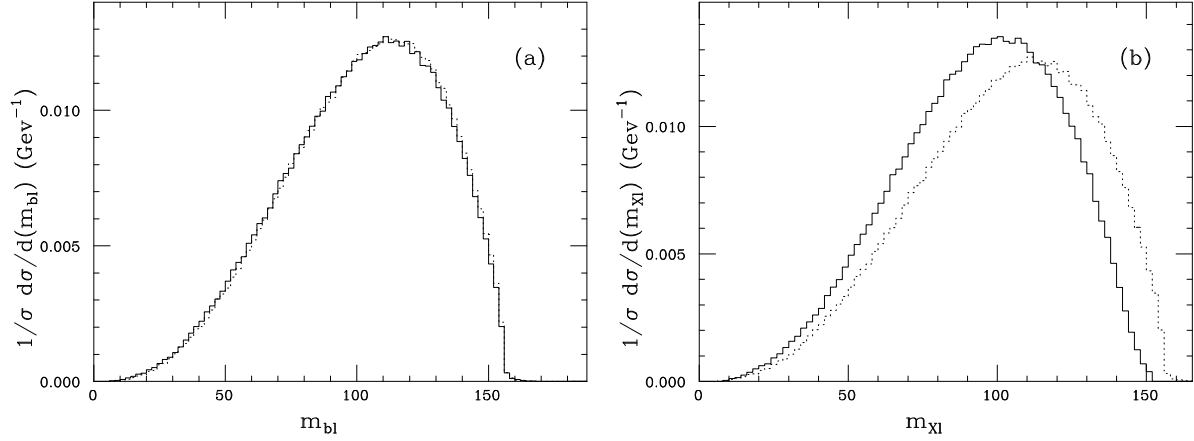


Figure 11: Distributions of the invariant mass of the b -lepton system for $m_t = 175$ GeV at the LHC according to HERWIG 6.1 (solid line) and 6.0 (dotted) (a) and according to 6.1, but at hadron-level ($X = B$, solid) and parton level ($X = b$, dotted) (b).

| m_t | $\langle m_{bl} \rangle^{6.1}$ | $\sigma(6.1)$ | $\langle m_{bl} \rangle^{6.0}$ | $\sigma(6.0)$ | $\langle m_{bl} \rangle^{6.0} - \langle m_{bl} \rangle^{6.1}$ |
|---------|--------------------------------|---------------|--------------------------------|---------------|---|
| 171 GeV | 99.19 GeV | 28.42 GeV | 99.81 GeV | 28.20 GeV | (0.627 ± 0.040) GeV |
| 173 GeV | 100.47 GeV | 28.84 GeV | 101.17 GeV | 28.43 GeV | (0.701 ± 0.041) GeV |
| 175 GeV | 101.76 GeV | 29.24 GeV | 102.48 GeV | 29.01 GeV | (0.718 ± 0.041) GeV |
| 177 GeV | 102.93 GeV | 29.67 GeV | 103.72 GeV | 29.43 GeV | (0.791 ± 0.042) GeV |
| 179 GeV | 104.36 GeV | 30.11 GeV | 104.99 GeV | 29.87 GeV | (0.628 ± 0.043) GeV |

Table 6: Results for the invariant mass m_{bl} at the LHC for different values of m_t .

5 Conclusions

We have studied $t\bar{t}$ events in the dilepton channel at the Tevatron and at the LHC using the new version of the HERWIG Monte Carlo event generator, which includes matrix-element corrections to the description of top decays. We considered observables involving the third hardest jet in transverse energy, to enhance possible effects of the implemented corrections.

We have found that the distributions obtained before and after matrix-element corrections are rather similar. A Kolmogorov test, which compares the shapes of two distributions, allows however to detect differences at the 95%CL with the large statistics available at the LHC. The statistics of the Run II at the Tevatron are however not sufficient.

We have also investigated the reconstruction of the top mass by looking at final states with leptons and a J/ψ . These final states are an excellent candidate for an experimental determination of the top mass with systematic errors in the range of 1 GeV. While the main production mechanisms of top quarks are different at the Tevatron and at the LHC, we found equivalent results in the two cases, indicating that this method of reconstruction of the top mass is not sensitive to the details of the colour-neutralisation model.

We considered the spectra of the invariant mass $m_{B\ell}$, where the B meson comes from the hadronisation of the b quark produced in $t \rightarrow bW$ and ℓ is the charged lepton from the decay $W \rightarrow \ell\nu$, for different values of m_t and obtained that the implementation of matrix-element corrections to top decays results in a shift of about 1.5 GeV on the top mass if one is able to reconstruct the whole $m_{B\ell}$ spectrum and of about 1 GeV after setting the cut $m_{B\ell} > 50$ GeV. The shifts we found are physical effects related to the inclusion of hard and large-angle gluon radiation in the Monte Carlo shower, since they are much larger than the statistical errors on them. Analyses at the parton level have shown an impact of a similar magnitude.

It will be now very interesting to compare the new HERWIG results for the invariant-mass distributions with the ones obtained after performing a next-to-leading order calculation of the process $t \rightarrow bWg$, and convoluting the result with the fragmentation function for the hadronisation of the b quark into a B meson taken from LEP and SLD data. In order to perform such a comparison in detail, the HERWIG cluster model used to simulate the hadronisation process will have to be tuned to fit that data.

Furthermore, although in this paper we have concentrated our analysis on the top mass reconstruction in final states with leptons and J/ψ , it will be worthwhile redoing the Tevatron analysis to determine m_t using the HERWIG parton shower model, provided with matrix-element corrections.

We finally recall that, though we feel safely confident that the new version of HERWIG will be a trustworthy event generator for the purpose top decays, top production is still performed in the soft/collinear approximation, with dead zones in the phase space which are needed to be filled. Matrix-element corrections to top production are in progress and may have an impact on jet observables and on the top mass measurement at the Tevatron as well.

Acknowledgements

We wish to acknowledge Bryan Webber for useful discussions on these and related topics. We thank A. Kharchilava for several discussions on the measurement of the top mass using the $\psi\ell$ final states. G.C. is also grateful to the R.A.L. Theory Group and to the CERN Theory Division for hospitality during some of this work.

References

1. S. Frixione, M.L. Mangano, P. Nason and G. Ridolfi, *Heavy Quark Production*, hep-ph/9702287, in *Heavy Flavours II*, ed. A.J. Buras and M. Lindner, World Scientific, p.609;
S. Frixione, M. L. Mangano, P. Nason and G. Ridolfi, Nucl. Phys. **B431** (1994) 453.
2. M. Beneke *et al.*, hep-ph/0003033, to appear in Proceedings of 1999 CERN Workshop on Standard Model Physics (and more) at the LHC, G. Altarelli and M.L. Mangano eds.
3. E. Accomando *et al.* [ECFA/DESY LC Physics Working Group Collaboration], Phys. Rept. **299**, 1 (1998) [hep-ph/9705442].
4. M. L. Mangano, P. Nason and G. Ridolfi, Nucl. Phys. **B373**, 295 (1992);
S. Frixione, M. L. Mangano, P. Nason and G. Ridolfi, Phys. Lett. **B351**, 555 (1995) [hep-ph/9503213].
5. M. Cacciari, M. Greco and P. Nason, JHEP **9805**, 007 (1998) [hep-ph/9803400];
F. I. Olness, R. J. Scalise and W. Tung, Phys. Rev. **D59**, 014506 (1999) [hep-ph/9712494].
6. G. Marchesini and B.R. Webber, Nucl. Phys. B310 (1988) 461. G. Marchesini et al., Comput. Phys. Commun. 67 (1992) 465.
7. T. Sjöstrand, Comp. Phys. Comm. 46 (1987) 367.
8. F. E. Paige and S. D. Protopopescu, BNL-29777; H. Baer, F. E. Paige, S. D. Protopopescu and X. Tata, ISAJET 7.48, hep-ph/0001086.
9. M.H. Seymour, Comput. Phys. Commun. 90 (1995) 95.
10. M.H. Seymour, Z. Phys. C56 (1992) 161.
11. M.H. Seymour, *Matrix Element Corrections to Parton Shower Simulation of Deep Inelastic Scattering*, contributed to 27th International Conference on High Energy Physics (ICHEP), Glasgow, 1994, Lund preprint LU-TP-94-12, unpublished.
12. G. Corcella and M.H. Seymour, Phys. Lett. B442 (1998) 417.
13. G. Corcella and M.H. Seymour, Nucl. Phys. B565 (2000) 227.
14. J. André and T. Sjöstrand, Phys. Lett. B442 (1998) 417
G. Miu and T. Sjöstrand, Phys. Lett. B449 (1999) 313.
15. A. Kharchilava, Phys. Lett. B476 (2000) 73.
16. G. Corcella, hep-ph/9911447, *On the Top Mass Reconstruction Using Leptons*, contributed to the U.K. Phenomenology Workshop on Collider Physics, Durham, U. K., 19-24 September 1999.
17. G. Marchesini and B.R. Webber, Nucl. Phys. B330 (1990) 261
18. G. Marchesini and B.R. Webber, Nucl. Phys. B238 (1984) 1.
19. G. Corcella, I.G. Knowles, G. Marchesini, S. Moretti, K. Odagiri, P. Richardson, M.H. Seymour, B.R. Webber, hep-ph/9912396.
20. L.H. Orr, T. Stelzer and W.J. Stirling, Phys. Rev. D56 (1997) 446

21. S. Catani, Yu.L. Dokshitzer, M.H. Seymour and B.R. Webber, Nucl. Phys. B406 (1993) 187
M.H. Seymour, Nucl. Phys. B421 (1994) 545.
22. S.D. Ellis and D.E. Soper, Phys. Rev. D48 (1993) 3160.
23. R. Bonciani, S. Catani, M.L. Mangano and P. Nason, Nucl. Phys. B529 (1998) 424.
24. The CDF II Detector, Technical Design Report, FERMILAB-Pub-96/390-E.
25. ATLAS detector and physics performance, Technical Design Report, Volume I, CERN LHCC 99-14.
26. K. Abe *et al.* [SLD Collaboration], hep-ex/9912058.